Electronic structure of bulk and multilayer black phosphorus under strain: a minimal model study

Mou Yang[1,3] and Hai Liu[2]

[1] Guangdong Provincial Key Laboratory of Quantum Engineering and Quantum Materials, School of Physics and Telecommunication Engineering, South China Normal University, Guangzhou 510006, People's Republic of China
[2] School of Computer Science, South China Normal University, Guangzhou 510006, People's Republic of China

E-mail: yang.mou@hotmail.com and liuhai@ecnu.edu.cn

CrossMark

Abstract

The tight-binding method is an important theoretical tool to investigate the physics of black phosphorus. Recently, a fifteen-parameter tight-binding model was proposed to precisely describe the band features. The large number of parameters is an obstacle for understanding the physics, and a minimal model for black phosphorus that grasps the main physics with satisfied precision is quite valuable. We use a tight banding model with only three parameters, that can reproduce the correct energy gap for monolayer, few-layer and bulk black phosphorus, to study the band structure black phosphorus under strain. The energy gap can be decreased by tensile strain normal to the phosphorus layers or in-plane compressive strain. At a certain critical strain, the gap of the phosphorus (either bulk, multilayer, or monolayer) is closed, and the dispersion is linear in the armchair direction and is parabolic in the other two principle directions. The simplicity of our model allows us to analytically investigate the energy gap and the critical strain as functions of the layer number of multilayer black phosphorus. When the strain exceeds the critical value, the valence and conduction bands evolve into two tents with their ridges touching each other.

Keywords: phosphorene, strain, tight-binding, electronic structure

(Some figures may appear in colour only in the online journal)

1. introduction

The ultra-thin layer black phosphorus, often called phosphorene, was exfoliated from its bulk counterpart recently [1]. Phosphorene draws much attention due to its great potential for application. It has a moderate direct band gap varying from 0.35 eV (the gap of bulk material) through 1.73 eV (the gap of monolayer material) [2], and the air exposure can slightly increase the band gap of few-layer phosphorene [3]. As a possible candidate of optoelectronic material, it may detect the entire visible spectrum of light and near-infrared light region [4, 5]. The optic absorption is highly polarized and it only active for the light polarized along armchair direction near the absorption edge [6, 7]. Phosphorene has high mobility and is regarded as an electronic material [8, 9]. Its field-effect transistors were demonstrated to have large on–off current ratio at room temperatures [10–12]. Few-layered phosphorene can accommodate edge bands on the zigzag edges, and these edge bands is sensitive to external electrical field [13, 14]. An insulator-semimetal transition can be caused by applying vertical strong electrical field [15–17], and such transition was verified in experiments [18–20]. Few-layered phosphorene is extreme flexible and can sustain large strain up to about 30% [21–23], that makes phosphorene a possible material for strain engineering.

---

[3] Author to whom any correspondence should be addressed.

Strain is a powerful tool to control the electronic structure of black phosphorus. It modifies the carrier mobility [24], tunes the band anisotropy [25], alters the transport properties [26], and induces the variation of the optical conductivity [27]. Strain can change the energy gap of phosphorene efficiently [28, 29], and many literatures reported that a critical strain can close the energy gap and turn phosphorene into a semi-Dirac semimetal material [30–36]. The strain induced signal of semi-Dirac semimetal material was already observed experimentally [37]. The transition, by taking into account the spin-orbital coupling, induces a few topological phases in phosphorene [38–40].

The tight-binding model is an important tool for theoretical research, and based on its parameter, the low-energy Hamiltonian can be derived, which is often adopted for analytically calculations [41–43]. The tight-binding parameters for phosphorene can be obtained by fitting its band structure to that of *ab intio* calculations [17, 45]. To properly describe the band features such as the band gap and the anisotropy, a lot of hopping parameters have to be used. ([17]) developed a tight-binding model with ten intra-layer hoppings and five inter-layer ones. It correctly reproduces the energy gap of monolayer, few-layer, and bulk back phosphorus reported in a recent measurement [2]. However, the large number of parameters leads to the difficulty to understand the physics and a minimal model for phosphorene, that can grasp the main physics and can reproduce the main results of experiments, is quite desired for theoretical research. Motivated by the above, we proposed a minimal tight-binding model that only has three nearest hopping parameters. Using the minimal model, we investigated the band structure of bulk and multilayer black phosphorus under the influence of strain. We analytically proved the effects verified by previous studies. The energy gap can be decreased by tensile strain normal to the phosphorus layers or in-plane compressive strain. At critical strain, the energy gap is closed, and the dispersion is linear in the armchair direction and is parabolic in zigzag direction and along the normal direction. In other words, strain can induce a 3D normal insulator semi-Dirac semimetal transition. We applied our model to multilayer phosphorene and obtained the critical strain as a function of the layer number of black phosphorus.

2. Bulk black phosphorus

The tight-binding Hamiltonian reads

$$H_{TB} = \sum_{i,j} t_{ij} c_i^+ c_j, \qquad (1)$$

where c_i (c_i^+) is the annihilation (creation) operator of electron on site i, t_{ij} is the hopping energy between sites i and j, and the summation runs over all site-pairs with nonzero hoppings. In this paper, only nearest neighborhood hoppings, including two types of intra layer hoppings and one type of inter layer hopping, are considered. The three types of hoppings are labeled as t_1, t_2 and t_3 in figure 1. When a strain is applied on the lattice, bond lengths are modified and thus the hoppings
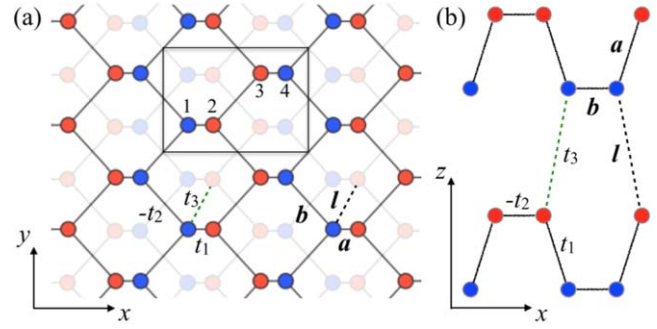

Figure 1. Sketch of top view and front view of black phosphorus lattice. The red and blue filled circles represent the puckered up and puckered down atoms.

Table 1. The geometry parameters [17] (in units of Å) and hopping energies without strain (in units of eV).

	a	*b*	*l*
x	0.7053	1.4797	0.7053
y	0	1.6550	1.6550
z	2.1261	0	3.1088
	t_1	t_2	t_3
	3.245	1.190	0.345

are changed correspondingly. The hopping energies are related to the corresponding bond lengths by the rule

$$\frac{t_\alpha}{t_\alpha^0} = \left(\frac{r_\alpha}{r_\alpha^0}\right)^{-2}, \quad \alpha = 1, 2, 3, \qquad (2)$$

where r_α are the bond length vectors corresponding to hopping energies t_α and the superscript 0 is used to denote the quantity without strain. We set the hopping parameters as shown in table 1 to ensure that the tight-binding calculation reproduces the correct energy gaps of monolayer, bilayer, and bulk black phosphorus materials, which were reported to be (in units of eV) 1.73, 1.15, 0.35 in a recent experimental measurement [2]. The bond lengths under strain are related with the unstrained ones and the stain by the relation

$$r_\alpha = r_\alpha^0 + (\epsilon_x r_{\alpha x}^0, \ \epsilon_y r_{\alpha y}^0, \ \epsilon_z r_{\alpha z}^0), \quad \alpha = 1, 2, 3, \qquad (3)$$

where $\epsilon_{x,y,z}$ are the strain components along x, y and z directions. The unstrained geometry parameters of black phosphorus are list in table 1.

We select four atoms labeled by 1 through 4 in figure 1 as the translational cell. The k-space Hamiltonian in basis of $|i\rangle$ ($i = 1, 2, 3, 4$) reads

$$\mathcal{H} = \begin{pmatrix} 0 & c_{12} & 0 & c_{14} \\ c_{12}^* & 0 & c_{14}^* & 0 \\ 0 & c_{14} & 0 & c_{34} \\ c_{14}^* & 0 & c_{34}^* & 0 \end{pmatrix} \qquad (4)$$

with the matrix elements defined by

$$c_{12} = t_1 e^{ik_x a_x} e^{ik_z a_z} + 2t_3 e^{ik_x a_x} \cos k_y b_y e^{-ik_z l_z},$$
$$c_{14} = -2t_2 e^{-ik_x b_x} \cos k_y d_y,$$
$$c_{34} = t_1 e^{ik_x a_x} e^{-ik_z a_z} + 2t_3 e^{ik_x a_x} \cos k_y b_y e^{ik_z l_z}. \quad (5)$$

To solve the eigen energies of the Hamiltonian, we introduce a set of unitary matrices

$$U_1 = \begin{pmatrix} e^{ik_x a_x} & & & \\ & 1 & & \\ & & e^{ik_x a_x} & \\ & & & 1 \end{pmatrix},$$

$$U_2 = \begin{pmatrix} e^{ik_z a_z} & & & \\ & 1 & & \\ & & 1 & \\ & & & e^{ik_z a_z} \end{pmatrix},$$

$$U_3 = \frac{1}{\sqrt{2}} \begin{pmatrix} 1 & 0 & 1 & 0 \\ 0 & 1 & 0 & 1 \\ 1 & 0 & -1 & 0 \\ 0 & 1 & 0 & -1 \end{pmatrix}. \quad (6)$$

By means of the unitary matrix $U = U_1 U_2 U_3$, we transform the Hamiltonian into

$$H = U^+ \mathcal{H} U = H_0 + V. \quad (7)$$

In the equation, the Hamiltonian H_0 describes the layered system without inter-layer coupling and it is a block diagonal matrix

$$H_0 = \begin{pmatrix} 0 & c_{12} & & \\ c_{12}^* & 0 & & \\ & & 0 & c_{34} \\ & & c_{34}^* & 0 \end{pmatrix} = \begin{pmatrix} h & \\ & h' \end{pmatrix}. \quad (8)$$

The matrix elements in the equation are renewed and are defined as

$$c_{12} = t_1 - 2(t_2 e^{-ik_x d_x} - t_3 \cos k_z d_z) \cos k_y d_y,$$
$$c_{34} = t_1 + 2(t_2 e^{-ik_x d_x} - t_3 \cos k_z d_z) \cos k_y d_y, \quad (9)$$

where $d_x = a_x + b_x$, $d_y = b_y$ and $d_z = l_z + a_z$. The lattice constants in x, y directions are $2d_x$ and $2d_y$, respectively, and that along z direction is d_z. The matrix V represents the inter-layer coupling and is a block anti-diagonal matrix

$$V = \begin{pmatrix} & & 0 & c_{14} \\ & & c_{14}^* & 0 \\ 0 & c_{14} & & \\ c_{14}^* & 0 & & \end{pmatrix} = \begin{pmatrix} & v \\ v^+ & \end{pmatrix}, \quad (10)$$

with

$$c_{14} = i2t_3 \cos k_y d_y \sin k_z d_z. \quad (11)$$

The energy gap occurs at Z point ($k_x = 0$, $k_y = 0$, $k_z = \pi/d_z$). At Z point, $c_{14} = 0$ and the conduction and valence band energies are totally determined by the matrix h. The conduction band bottom is

$$E_C(Z) = |c_{12}| = t_1 - 2(t_2 + t_3). \quad (12)$$

Because of the electron–hole symmetry, the valence band top is $E_V = -E_C$, and so the energy gap reads

$$E_g = 2|t_1 - 2(t_2 + t_3)|. \quad (13)$$

When no strain is applied on the system, we have $t_1 > 2(t_2 + t_3)$ and $E_g = 0.35$eV.

If the lattice is suffered by a tensile strain along z direction, a_z is enlarged, t_1 is thus decreased, and the energy gap shrinks (The parameter t_3 is also decreased, while the change of t_3 is less important since t_1 is about 10 times of t_3). If a compressive strain in either x- or y-direction is applied, the length of $\boldsymbol{b}$ is shortened, t_2 becomes larger, and the energy gap decreases. There is a critical strain (in-plane compressive or vertical tensile strain) can be found to vanish the energy gap. At the critical strain, the hoppings satisfy the relation

$$t_1 = 2(t_2 + t_3). \quad (14)$$

According to the equation, the critical strains in x, y and z directions are calculated to be -0.108, -0.058 and 0.038, respectively. One can see that the in-plane compressive strains make the energy gap shrink and the y direction is the easy axis for gap modification, which are consistent with known results [36, 45]. These critical values are quite close to those obtained from the fifteen-parameter tight-binding model [17], which predicts the critical strains to be -0.117, -0.057 and 0.039 respectively[4].

If no strain is applied or the strain is not large to reach the critical value, the dispersion is of parabolic type at the vicinity of Z point along any direction, as showed in the left column of figure 2. When a critical strain is applied and the energy gap is closed, there are interesting features in the dispersions along three principle directions cross Z point. We set $k_x \to 0$ and have

$$E_C = |c_{12}| = |t_1 - 2(t_2 e^{-ik_x d_x} + t_3)|$$
$$= 2t_2 |d_x k_x|, \quad (15)$$

in which the relation equation (14) is used. The above equation implies that the dispersion in x direction across Z point is linear. The dispersion along y direction at Z point can be obtained by letting $k_y \to 0$,

$$E_C = |c_{12}| = |t_1 - 2(t_2 + t_3) \cos k_y d_y|$$
$$= (t_2 + t_3)(d_y k_y)^2. \quad (16)$$

One can see the dispersion in y direction is parabolic. When we consider the dispersion in z direction, we replace k_z with $k_z + \pi/d_z$ and set $k_z \to 0$. For this case, the inter-layer coupling matrix V cannot be ignored. The reduced Hamiltonian of the conduction and valence bands can be obtained as

$$H_{CV} = h + v \frac{1}{E - h'} v^+ = h - v \frac{1}{h'} v^+, \quad (17)$$

where h, h' and v are matrices appearing in equations (8) and (10). Applying equation (14) and solving the eigen values, we

---

[4] The k-space Hamiltonian of bulk black phosphorus of the fifteen-parameter model is $H = H_M + (H_C e^{-ik_z d_z} + \text{c.c.})$, where H_M and H_C are the matrices given in equation (4) in ([35]). Supposing the hoppings depend on the bond length by equation (2), we obtain the band structure. Tuning the strain so as to close the band gap, we can find the critical strains.
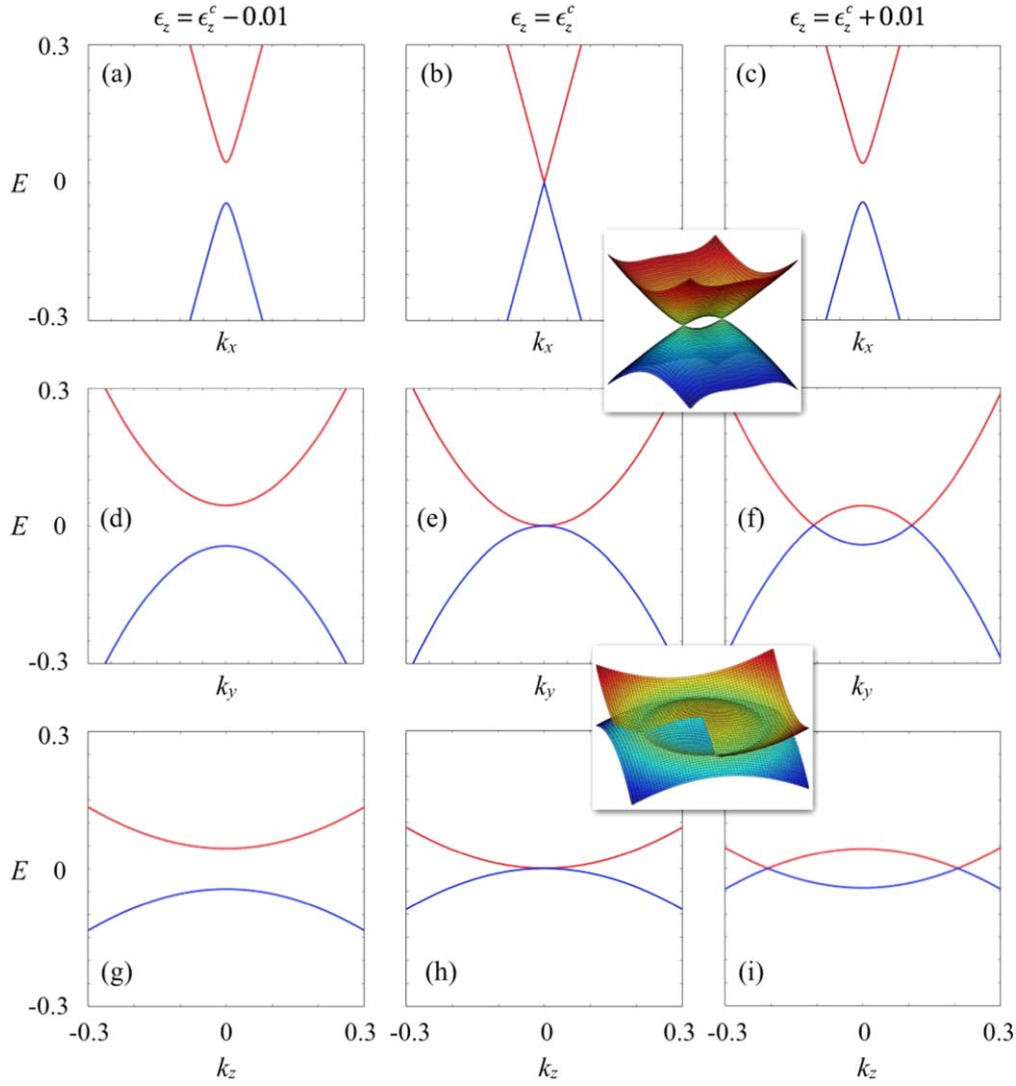
Figure 2. The band energies (in units of eV) as functions of wavevector (in units of π/d_α, $\alpha = x, y, z$) across Z point. The upper and lower insets show respectively the 3D band structures for $k_z = 0$ and for $k_x = 0$ under strain $\epsilon_z = \epsilon_z^c + 0.01$.

have the conduction band energy

$$E_C = (1 + \eta)t_3(d_z k_z)^2, \tag{18}$$

where $\eta = t_3/(t_2 + t_3)$. The dispersion in z direction is parabolic. Because t_3 is much smaller than t_2, the effective mass along z direction is much larger than that in y direction. The middle column of figure 2 shows the dispersions in the principle directions across Z point and demonstrates the features as we discussed: the dispersion is linear along x direction and is parabolic in other directions.

If the strain exceeds the critical value, the conduction band bottom in equation (12) is negative. We define $\delta t = 2(t_2 + t_3) - t_1 > 0$. The dispersion features near Z point can be obtained by the proceeding the above analysis all over again. In x direction, the conduction dispersion reads

$$E_C = |t_1 - 2(t_2 e^{-ik_x d_x} + t_3)|$$
$$= \delta t + \frac{2t_2^2}{\delta t}(d_x k_x)^2. \tag{19}$$

The dispersion in x direction recovers to its typical parabolic

type with the energy gap $2\delta t$, as showed in figure 2(c). In y direction, we have

$$E_C = |t_1 - 2(t_2 + t_3)\cos k_y d_y|$$
$$= \delta t - (t_2 + t_3)(d_y k_y)^2. \tag{20}$$

The dispersion is of parabolic type and it opens downward, as figure 2(f) shows. The energy gap at Z point is $2\delta t$, and it will be closed at some points besides Z point. The inset illustrates what the band structure on the k_x–k_y plane looks like. Around the band touching points, the dispersion is linear, as that in graphene. In z direction, we have

$$H_{CV} = h + v\frac{1}{E - h'}v^+ = h + v\frac{1}{\delta t - h'}v^+. \tag{21}$$

By regarding δt as a small quantity, we have the conduction band dispersion

$$E_C = \delta t - (1 + \eta)t_3(d_z k_z)^2. \tag{22}$$

It is also an inverse parabolic curve. Figure 2(i) shows the situation and the inset demonstrates the band structure on

k_y–k_z plane. The conduction and valence bands touch with each other on a ring, and a cavity forms between them.

The minimal tight-binding Hamiltonian has electron–hole symmetry. Supposing the conduction and valence band energies detected experimentally are ϵ_C and ϵ_V respectively, the average of them $\epsilon_{av} = (\epsilon_C + \epsilon_V)/2$ is a quantity to reflect the electron–hole asymmetry. The Hamiltonian

$$H_{\text{asym}} = H + \epsilon_{av} \tag{23}$$

not only reflects electron–hole asymmetry, but also describes the anisotropy of effective mass, and therefore is a good model to describe the physics near Z point.

3. Multilayer phosphorene

For the multilayer phosphorene having N layers, k_z is not a good quantum number but a parameter to characterize the subbands. We assume that the wavefunction vanishes on the layer just beneath and above the multilayer system. This requires that k_z are quantized as

$$k_z = \frac{n\pi}{(N+1)d_z}, \quad n = 1, 2, \cdots, N. \tag{24}$$

The energy gap takes place at Γ point ($k_x = 0$ and $k_y = 0$) when k_z takes the value most close to π/d_z, saying the value when $n = N$. For this case, we have

$$k_z d_z = \pi - \theta, \tag{25}$$

where $\theta = \pi/(N+1)$. At Γ point, the matrix elements in equations (9) and (11) are renewed as

$$
\begin{aligned}
c_{12} &= t_1 - 2(t_2 + t_3 \cos\theta), \\
c_{34} &= t_1 + 2(t_2 + t_3 \cos\theta), \\
c_{14} &= i2t_3 \sin\theta.
\end{aligned} \tag{26}
$$

The energy gap can be analytically calculated to be

$$E_g = 2\sqrt{t_1^2 + 4t_3^2 \sin^2\theta} - 4(t_2 + t_3 \cos\theta). \tag{27}$$

The equation indicates the function of energy gap versus layer number. By tuning the applied strain to letting $E_g = 0$, we have the critical strain as function of layer number. If we set $N = \infty$, we have $\sin\theta = 0$ and $\cos\theta = 1$, and the equation is reduced to equation (13).

The monolayer case can be easily obtained by setting $t_3 = 0$ and the result is $E_g = 2(t_1 - 2t_2)$, which produces the result 1.73 eV. The critical strain can be found when $t_1 = 2t_2$ is satisfied.

Figures 3(a) and (b) show the curves of energy gap and critical strain versus layer number. The energy gap decreases with the layer number and the critical strain decays as similar way. For black phosphorus with a few tens of layers, the energy gap and critical strain tend to be those of the bulk material. Figures 3(c)–(e) demonstrate the lowest conduction bands and highest valence band of a 50-layer black phosphorus. When the strain does not exceed the critical strain, the material is a normal semiconductor. When the strain equals the critical strain, the band touching happens and the dispersion in x-direction is parabolic and linear in y-direction. If
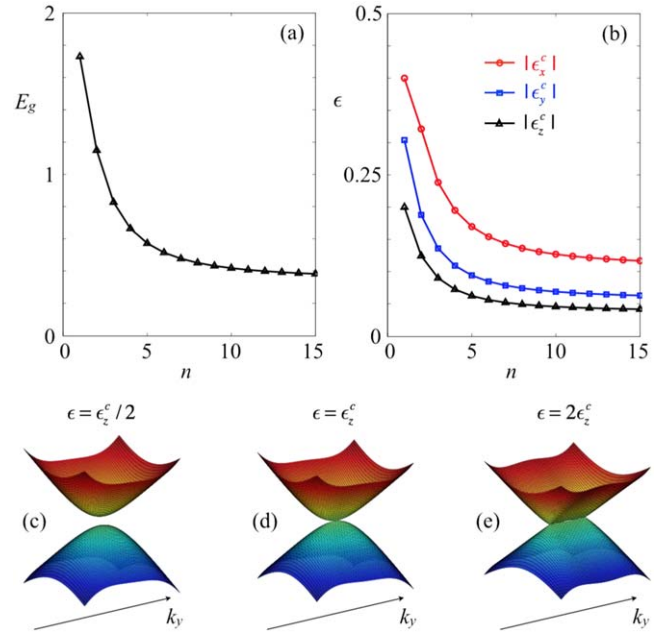

Figure 3. (a) Energy gap as a function of layer number. (b) Magnitude of critical strain along x, y, and z directions versus layer number. (c)–(e) Lowest conduction band and highest valence band under different strains along z direction for 50 layers of black phosphorus.

the strain exceeds the critical strain, the band inversion happens and different conduction and valence subbands cross at different values of k_y. For the layer number $N \gg 1$, the subband-cross points form a line, and the lowest conduction and highest valence bands look like two camping tents with their ridges touched.

4. Summary

We proposed a three-hopping nearest-neighborhood tight-binding model to study the band structure and that under strain. We showed that strain can induce an insulator-semi-Dirac semimetal transition in both bulk black phosphorus and few-layer phosphorene. By virtue of the simplicity of our model, the features of semi-Dirac bands were identified analytically. The value of critical strain for the transition as a function of the layer number of multilayer phosphorene was obtained and it coincides with that of the fifteen-parameter model. Our model, which is simple and reproduces the main physics under strain, can be used as a convenient platform for theoretical research.

Acknowledgments

ORCID iDs

Mou Yang ⓘ https://orcid.org/0000-0002-3716-0652

References

[1] Xia F, Wang H and Jia Y 2014 *Nat. Commun.* **5** 4458
[2] Li L *et al* 2017 *Nat. Nanotechnol.* **12** 21
[3] Wang F, Zhang G, Huang S, Song C, Wang C, Xing Q, Lei Y and Yan H 2019 *Phys. Rev. B* **99** 075427
[4] Youngblood N, Chen C, Koester S J and Li M 2015 *Nat. Photon.* **9** 247
[5] Buscema M, Groenendijk D J, Blanter S I, Steele G A, van der Zant H S J and Castellanos-Gomez A 2014 *Nano Lett.* **14** 3347
[6] Tran V, Soklaski R, Liang Y and Yang L 2014 *Phys. Rev. B* **89** 235319
[7] Duan H, Yang M and Wang R 2016 *Physica* E **81** 177
[8] Liu H, Neal A T, Zhu Z, Luo Z, Xu X, Tománek D and Ye P D 2014 *ACS Nano* **8** 4033
[9] Rudenko A N, Brener S and Katsnelson M I 2016 *Phys. Rev. Lett.* **116** 246401
[10] Li L, Yu Y, Ye G J, Ge Q, Ou X, Wu H, Feng D, Chen X H and Zhang Y 2014 *Nat. Nanotechnol.* **9** 372
[11] Koenig S P, Doganov R A, Schmidt H, Neto A H and Özyilmaz B 2014 *Appl. Phys. Lett.* **104** 103106
[12] Yin D and Yoon Y 2016 *J. Appl. Phys.* **119** 214312
[13] Ezawa M 2014 *New J. Phys.* **16** 115004
[14] Yang M, Duan H-J and Wang R-Q 2015 *JETP Lett* **102** 610
[15] Yuan S, van Veen E, Katsnelson M I and Roldán R 2016 *Phys. Rev. B* **93** 245433
[16] Liu Q, Zhang X, Abdalla L B, Fazzio A and Zunger A 2015 *Nano Lett.* **15** 1222
[17] Rudenko A N, Shengjun Yuan and Katsnelson M I 2015 *Phys. Rev. B* **92** 085419
[18] Kim J, Baik S S, Ryu S H, Sohn Y, Park S, Park B-G, Denlinger J, Yi Y, Choi H J and Kim K S 2016 *Science* **349** 723
[19] Kim J, Baik S S, Jung S W, Sohn Y, Ryu S H, Choi H J, Yang B-J and Kim K S 2017 *Phys. Rev. Lett.* **119** 226801
[20] Ehlen N, Sanna A, Senkovskiy B V, Petaccia L, Fedorov A V, Profeta G and Grüneis A 2018 *Phys. Rev. B* **97** 045143
[21] Verma D, Hourahine B, Frauenheim T, James R D and Dumitrică T 2016 *Phys. Rev. B* **94** 121404
[22] Wei Q and Peng X 2014 *Appl. Phys. Lett.* **104** 251915
[23] Peng X, Wei Q and Copple A 2014 *Phys. Rev. B* **90** 085402
[24] Priydarshi A, Chauhan Y S, Bhowmick S and Agarwal A 2018 *Phys. Rev. B* **97** 115434
[25] Arra S, Babar R and Kabir M 2019 *Phys. Rev. B* **99** 045432
[26] Nourbakhsh Z and Asgari R 2018 *Phys. Rev. B* **98** 125427
[27] Yang C H, Zhang J Y, Wang G X and Zhang C 2018 *Phys. Rev. B* **97** 245408
[28] Jiang J-W and Park H S 2015 *Phys. Rev. B* **91** 235118
[29] Rodin A S, Carvalho A and Neto A H C 2014 *Phys. Rev. Lett.* **112** 176801
[30] Gong P-L, Liu D-Y, Yang K-S, Xiang Z-J, Chen X-H, Zeng Z, Shen S-Q and Zou L-J 2016 *Phys. Rev. B* **93** 195434
[31] Fei R, Tran V and Yang L 2015 *Phys. Rev B* **91** 195319
[32] Elahi M, Khaliji K, Mohammad S, Pourfath M and Asgari R 2015 *Phys. Rev. B* **91** 115412
[33] Pietro P D *et al* 2018 *Phys. Rev. B* **98** 165111
[34] Guan J, Song W, Yang L and Tománek D 2016 *Phys. Rev. B* **94** 045414
[35] He S, Yang M and Wang R-Q 2018 *Chin. Phys. B* **27** 047303
[36] Zhang T, Lin J-H, Yu Y-M, Chen X-R and Liu W-M 2015 *Sci. Rep.* **5** 13927
[37] Xiang Z J *et al* 2015 *Phys. Rev. Lett.* **115** 186403
[38] Sisakht E T, Fazileh F, Zare M H, Zarenia M and Peeters F M 2016 *Phys. Rev. B* **94** 085417
[39] Zhao J, Yu R, Weng H and Fang Z 2016 *Phys. Rev. B* **94** 195104
[40] Liu H, Sun J-T, Cheng C, Liu F and Meng S 2018 *Phys. Rev. Lett.* **120** 237403
[41] Pereira J M Jr and Katsnelson M I 2015 *Phys. Rev. B* **92** 075437
[42] Mogulkoc A, Mogulkoc Y, Rudenko A N and Katsnelson M I 2016 *Phys. Rev. B* **93** 085417
[43] Mogulkoc A, Modarresi M and Rudenko A N 2017 *Phys. Rev. B* **96** 085434
[44] Rudenko A N and Katsnelson M I 2014 *Phys. Rev. B* **89** 201408
[45] Zhang R-Y, Zheng J-M and Jiang Z-Y 2018 *Chin. Phys. Lett.* **35** 017302